

Supplementary information

X-ray micro-computed tomography-based approach to estimate the upper limit of natural H₂ generation by Fe²⁺ oxidation in the intracratonic lithologies

Kanchana Kularatne^{a,b*}, Pascale Sénéchal^b, Valentine Combaudon^{a,b,d}, Othmane Darouich^b, Maria Angels Subirana^e, Arnaud Proietti^f, Caroline Delhay^g, Dirk Schaumlöffel^e, Olivier Sissmann^c, Eric Deville^c, Hannelore Derluyn^a

^aUniversite de Pau et des Pays de l'Adour, E2S UPPA, CNRS, LFCR, Pau, France

^bUniversite de Pau et des Pays de l'Adour, E2S UPPA, CNRS, DMEX, Pau, France

^cIFP Energies Nouvelles, 1- 4 Avenue du Bois Préau, 92852 Rueil-Malmaison, France

^dDepartment of Geological Sciences, University of Colorado, Boulder, CO 80309, USA

^eUniversité de Pau et des Pays de l'Adour, CNRS, Institut des Sciences Analytiques et de Physico-Chimie pour l'Environnement et les Matériaux (IPREM), UMR 5254, Helioparc, 2 Avenue Pierre Angot, 64053, PAU, France

^fCentre de Microcaractérisation Raimond Castaing, 3 Rue Caroline Aigle, 31400 Toulouse, France

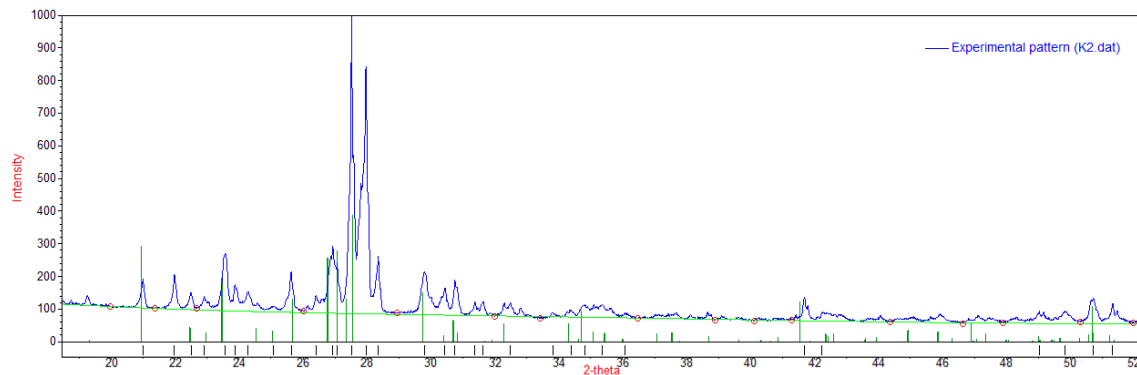
^gUniversité Bordeaux 1, Institut des Sciences Moléculaires (ISM) UMR 5255, 351 Cours de la libération, 33405 Talence Cedex, France

*corresponding author: kanchana.kularatne@univ-pau.fr

Contents

#	Supplementary information	Page
SI.1	XRD powder analysis of the monzo-diorite sample.....	2
SI.2	Parameters used for calculation of LAC's	2
SI.3	SEM EDS element distribution of Na, K, Fe, Ti, Ca, and Mg.....	2
SI.4	Micro-Raman analysis: locations of point analysis and spectra.....	3
SI.5	Histogram of grey values	4
SI.6	Phase segmentation in large samples.....	4
SI.7	SEM BSE images of veins.....	6
SI.8	NanoSIMS analysis on the fractures within fayalite	7
SI.9	NanoSIMS analysis on the fractures within feldspar.....	7
SI.10	Chemical formulae, molar masses and densities of minerals.....	8
SI.11	Theoretical linear attenuation coefficients (LACs) of the minerals appearing in Eq.2 to 15 as a function of X-ray energy	8

SI. 1. XRD powder analysis of the monzo-diorite sample

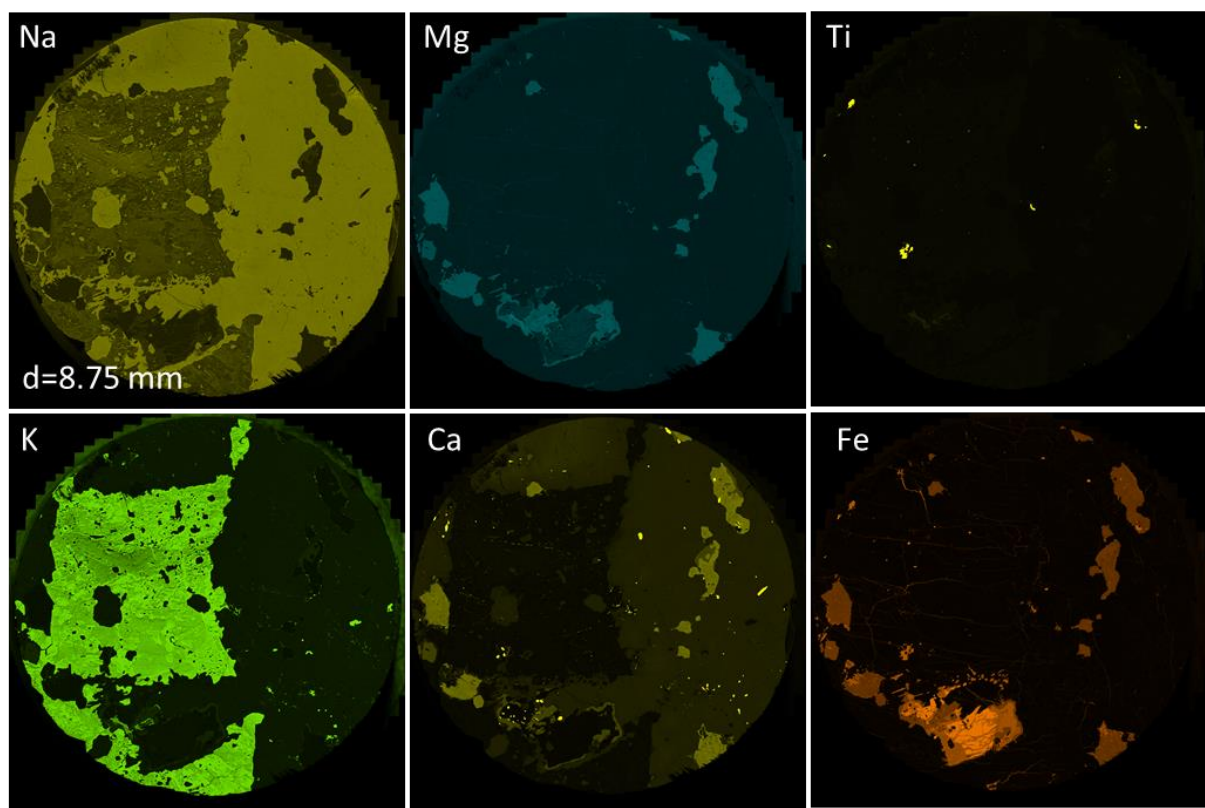


SI.2. Parameters used for calculation of LAC's

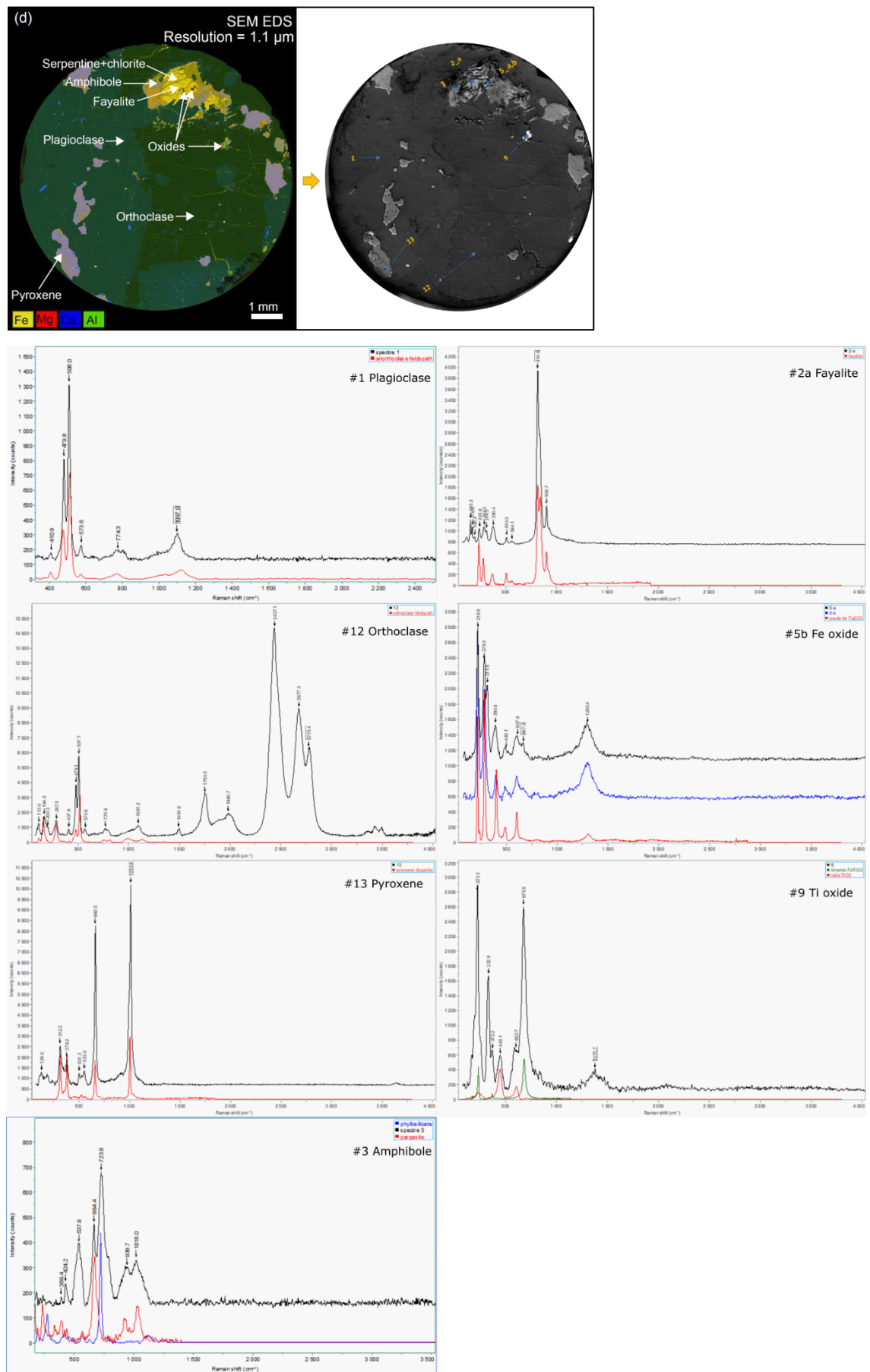
Mineral	General formula*	Formula used in material creator	Molar mass (g/mol)	Density (g/cm ³)*
Olivine	Mg ₂ FeSiO ₄		153.31	3.30
Serpentine (crysoltite)	Mg ₃ Si ₂ O ₅ (OH) ₄		277.11	2.59
Brucite	Mg(OH) ₂		58.32	2.37
Magnetite	Fe ₃ O ₄		231.54	5.15
Pyroxene (ferrosilite)	FeMgSi ₂ O ₆		232.32	3.95
Fayalite	Fe ₂ SiO ₄		203.78	4.39
Siderite	FeCO ₃		115.86	3.87
Hematite	Fe ₂ O ₃		159.69	5.30
Pyrite	FeS ₂		119.98	5.01
Biotite	K(Mg,Fe) ₃ [AlSi ₃ O ₁₀ (OH,F) ₂]	KMg ₁ Fe ₂ AlSi ₃ O ₁₀ OH ₂	433.53	3.10
Arfvedsonite	NaNa ₂ (Fe) ₅ Si ₈ O ₂₂ (OH) ₂	NaNa ₂ Fe ₅ Si ₈ O ₂₂ O ₂ H ₂	958.89	3.45
Aegirine	NaFeSi ₂ O ₆		231.00	3.52
Goethite	FeO(OH)		88.85	4.27
Chlorite (chamosite)	(Fe,Mg)5Al(Si ₃ Al)O ₁₀ (OH,O) ₈	Fe ₅ AlSi ₃ AlO ₁₀ O ₈ H ₈	664.18	3.13
Amphibole(Fe-pargasite)	NaCa ₂ (Fe ₄ Al)(Si ₆ Al ₂)O ₂₂ (OH) ₂	KCa ₂ Fe ₄ AlSi ₆ Al ₂ O ₂₂ O ₂ H ₂	961.99	3.13
Ilmanite (Fe-Oxide)	FeTiO ₃		151.73	4.79
Orthoclase	KAlSi ₃ O ₈		278.33	2.55
Plagioclase	(Na,Ca)(Si,Al) ₄ O ₈		270.77	2.69

*mineral densities obtained from webminerals

SI.3. SEM EDS element distribution of Na, K, Fe, Ti, Ca, and Mg

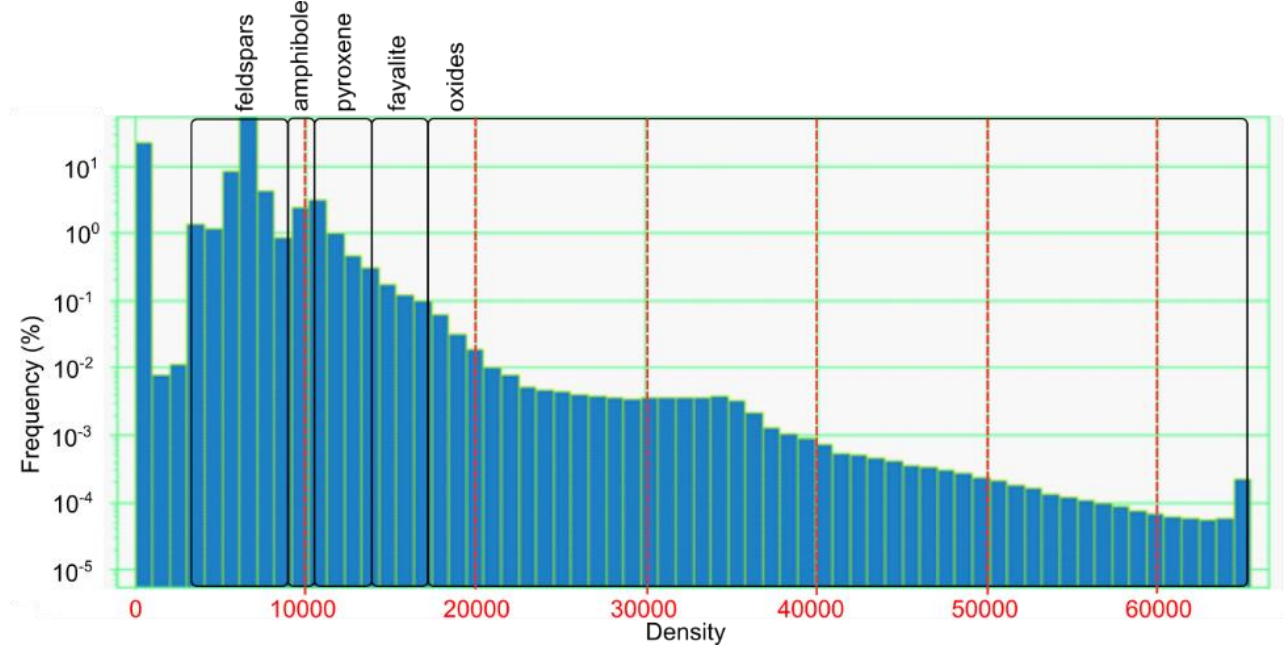


SI.4. Micro-Raman analysis: locations of point analysis and spectra



SI.5. Histogram of grey values

Figure below shows the histogram of grey values corresponding to the 2D micro-CT slice shown in Fig.3b. The first peak represents the grey value of the background (grey value=0), then approximately 5-6 peaks can be identified which correspond to phases present in the sample.



SI.6. Phase segmentation in large samples

A summary of micro-CT analysis performed on five gabbro samples are given in the table below. The sample K2_d8-a (top) is the one used to develop the workflow given in Fig.1. The four other samples are larger samples with volumes varying between 511.92 mm^3 – 18756.39 mm^3 . These samples were imaged at higher voxel sizes up to $30 \mu\text{m}$. The aim was to segment two phases (1) feldspar (2) mineral clusters as a whole. Here we report the volume of whole sample ($V_{(\text{Sample})}$), volume of feldspar ($V_{(\text{Feldspar})}$) and the volume of mineral cluster (pyroxene+fayalite+amphibole+oxides) ($V_{(\text{Cluster})}$). Then for each sample, we obtained the percentage volume of mineral cluster and feldspar. The results show that the percentage volume of mineral cluster and feldspar are coherent in the samples with larger volumes compared to the K2_d8-a (top). Using these data, we calculated the average volume % of mineral cluster (18.50 vol.%) and the average volume % of feldspar (81.50 vol.%). As we already know the volume percentages of individual minerals in a cluster from the analysis of the K2_d8-a (top) sample, we could upscale it to the larger sample volume with 18.5 vol.% clusters and 81.5 vol.% of feldspar, as given in table SI.2.2.

Table. SI.2.1. Summary of micro-CT analysis on the five samples and volumes of phases obtained

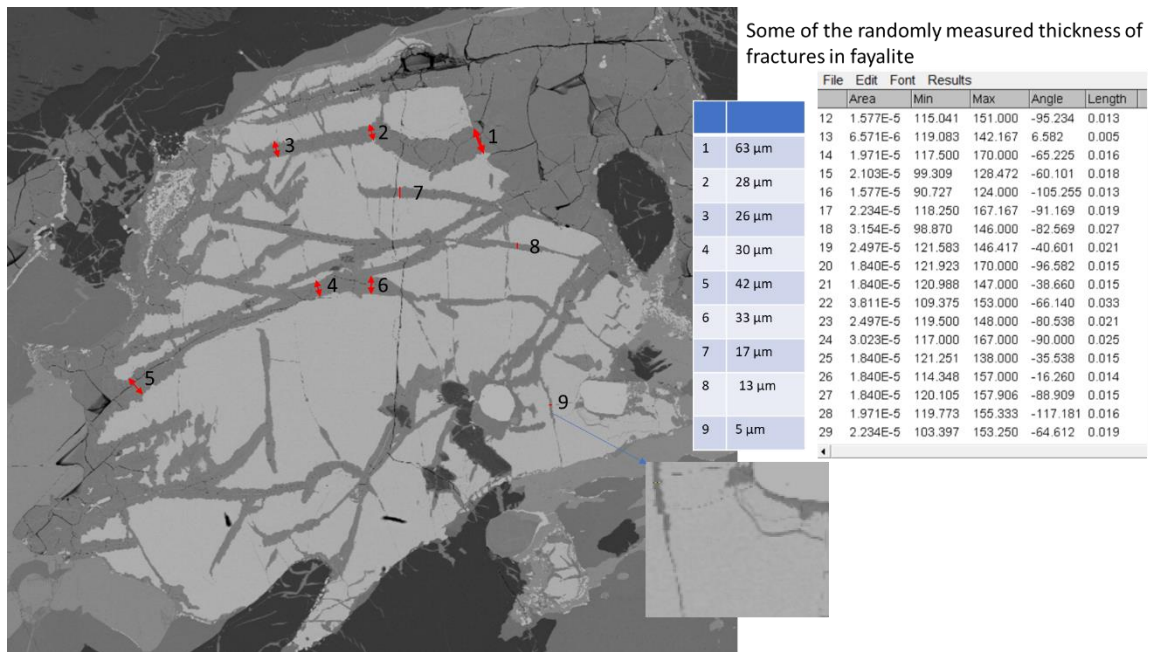
	K2_d8-a (top)	K2_d8-b (global)	K2_d8 (full core)	K2_d20	K2_block	Average
Scanner	TESCAN	TESCAN	BRUKER	TESCAN	TESCAN	-
Energy	60 kV	60 kV	70 kV	160 kV	140 kV	-
Voxel size (μm)	3.5	3.5	6	10	30	-
$V_{(\text{Sample})}$ (mm^3)	217.5	511.92	944.62	3254.94	18756.39	-
$V_{(\text{Feldspar})}$ (mm^3)	193.71	412.83	777.19	2696.74	15052.46	-
$V_{(\text{Cluster})}$ (mm^3)	23.79	99.09	167.43	558.2	3703.93	-
Cluster vol.%	10.94	19.36	17.72	17.15	19.75	18.50
Feldspar vol.%	89.06	80.64	82.28	82.85	80.25	81.50

Table. SI.2.2. Recalculated mineral vol.% for the sample with average volume (18.50 vol.% of clusters and 81.50 vol.% of feldspar)

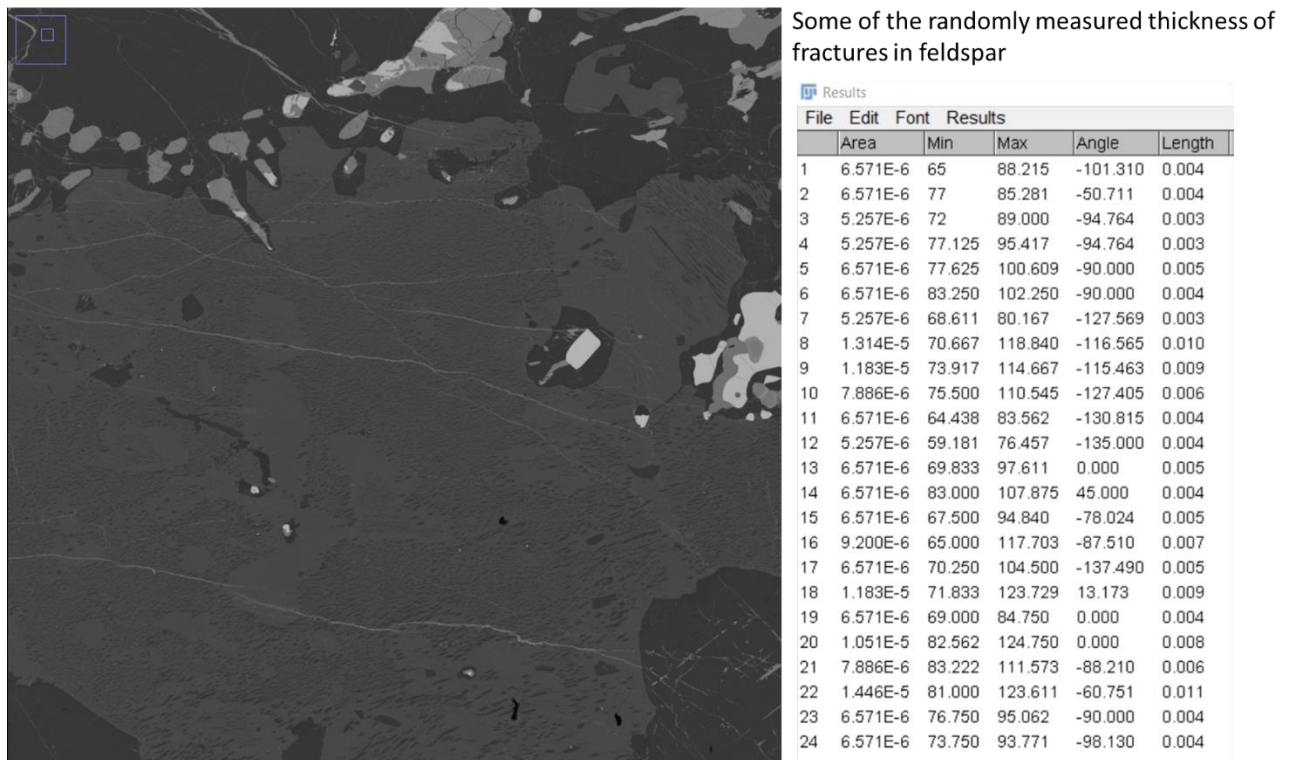
	K2d8-a (top)		\pm uncertainty
	Vol.% minerals within a cluster	Vol.% minerals within the full sample	
Feldspar	-	81.50	1.26
Amphibole	28.72	5.31	0.36
Pyroxene	61.53	11.38	0.77
Fayalite	7.02	1.30	0.09
oxides	2.73	0.50	0.03
	100	100	

SI.7. SEM BSE images of fractures

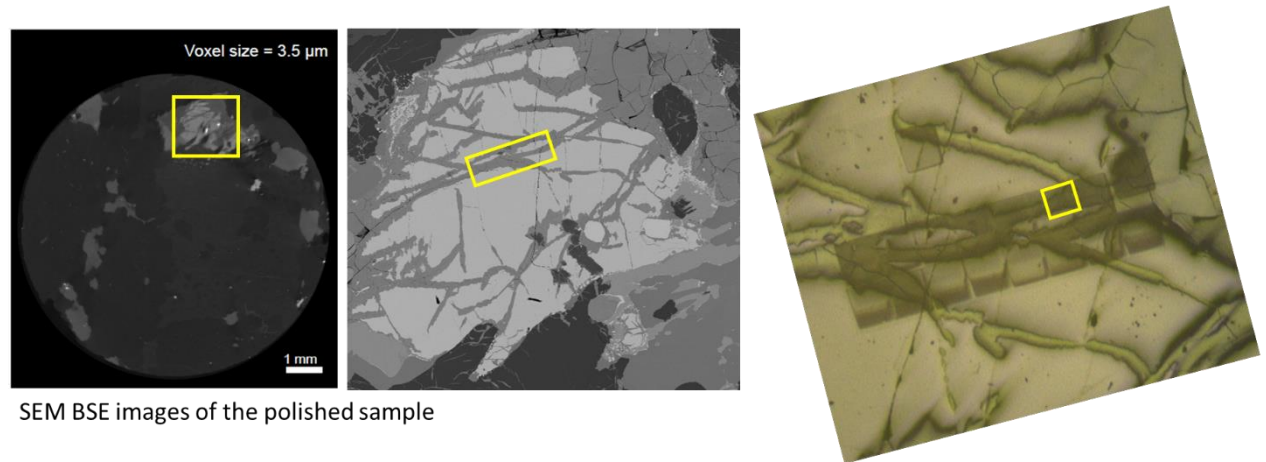
SEM BSE image showing fractures in a fayalite grain. FIJI software was used to measure the thickness of the fractures. The thickest fractures are marked on the figure (numbered 1-9) and their thicknesses are given in μm . The last column (Length) in the adjacent table gives the thicknesses of randomly measured fractures in mm. The average thickness of fractures within fayalite is taken as $18 \mu\text{m}$.



SEM BSE image showing fractures in a feldspar. The last column of table shows the thicknesses of the fractures in mm. The avrage thickness of fractures within feldspar was taken to be $5 \mu\text{m}$.

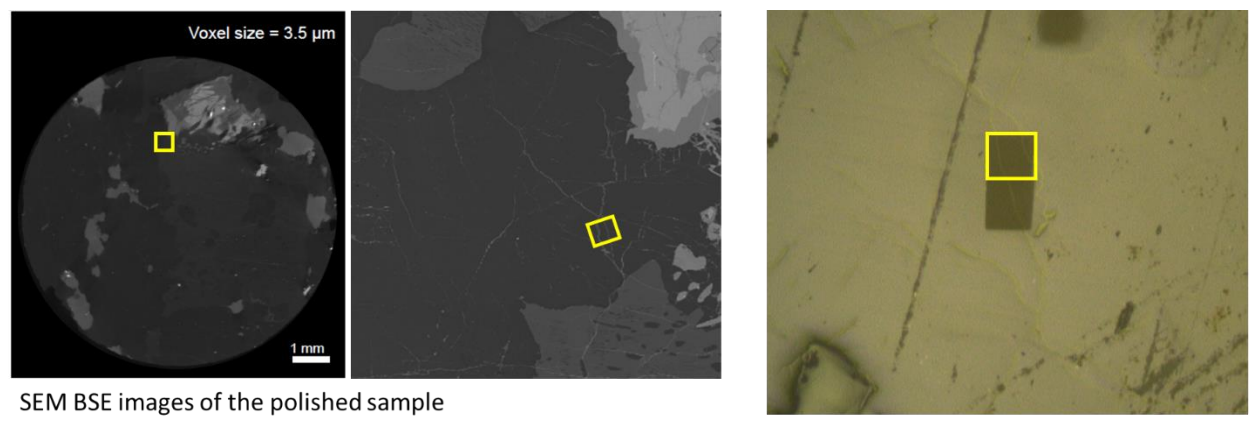


SI.8. Fractured fayalite grain showing the exact location of nanoSIMS analysis



Microscopy image showing spots of nanoSIMS analysis. The yellow square shows the exact spot of the element maps shown in Fig.3c.

SI.9. Fractured feldspar in the sample showing the exact location of nanoSIMS analysis



Microscopy image showing spots of nanoSIMS analysis. The yellow square shows the exact spot of the element maps shown in Fig.3f.

SI. 10. Chemical formulae, molar masses and densities of minerals present in monzo-diorite from Kansas, USA

Mineral	Chemical formula	Molar mass (gmol ⁻¹)	Density (gcm ⁻³)
Plagioclase	Na _{0.8} Al _{0.2} Ca _{0.2} Si _{2.8} O ₈	238.44	2.62
Orthoclase	K _{0.8} Na _{0.2} AlSi ₃ O ₈	275.11	2.56
Pyroxene	FeCa _{0.7} Mg _{0.3} Si ₂ O ₆	631.40	3.95
Amphibole	Fe _{3.5} Al _{1.9} Ca _{1.7} Mg _{1.1} Na _{0.4} K _{0.2} Si ₆ O ₂₂	879.11	3.17
Fayalite	Fe ₂ SiO ₄	203.77	4.39
Oxides	*FeTiO ₃	151.71	5.20
Serpentine	*Fe ₃ Si ₂ O ₅	371.7	3.35
Chlorite	*Mg ₅ Al(AlSi ₃ O ₁₀)(OH) ₈	555.80	2.60

*Generalized formulae

SI.11. Theoretical linear attenuation coefficients (LACs) of the minerals appearing in Eq.2 to 15 as a function of X-ray energy

